Development and Experimental Testing of a FEM Model for the Stress Distribution Analysis in Agricultural Soil due to Artificial Compaction

Sorin-Ştefan BIRIŞ [1](✉)
Valentin VLĂDUŢ [2]
Nicoleta UNGUREANU [1]
Gigel PARASCHIV [1]
Gheorghe VOICU [1]

Summary

It is known that the compaction phenomenon of agricultural soil can be defined as an increase in its dry density, respectively as in reduction of its porosity, and it can result from any natural causes as: rainfall impact, soaking, internal water stress from soil, and other. An important role has the artificial compaction, which is generated by the contact with tyres or caterpillars of tractors and agricultural machines. In present, one of the most advanced methods for modelling the phenomenon of stresses propagation in agricultural soil is the Finite Element Method (FEM), which is a numerical method for obtaining approximate solutions of ordinary and partial differential equations of this distribution. In this paper, the soil has been idealised as an elastic-plastic material by Drucker-Prager yield criteria. This paper presents a model for prediction of the stress state in agricultural soil below agricultural tyres in the driving direction and perpendicular to the driving direction, which are different from one another, using the Finite Element Method. General model of analysis was created using FEM, which allows the analysis of equivalent stress distribution and the total displacements distribution in the soil volume, making evident both of the conditions in which the soil compaction is favour and of the study of graphic variation of equivalent stress and the study of shifting in the depth of the soil volume. Using an acquisition data system and pressure sensors, the theoretical model was experimentally checked in the laboratory

Key words

soil compaction, finite element method, stress state, tractor, tyre

[1] Politehnica University of Bucharest, Faculty of Biotechnical Systems Engineering, Department of Biotechnical Systems, Splaiul Independentei 313, 060042, Bucharest, Romania
✉ e-mail: biris.sorinstefan@gmail.com
[2] National Institute of Research-Development for Machines and Installations Designed for Agriculture and Food Industry – INMA, Str. Ion Ionescu de la Brad., No. 6, S. 1, Bucharest, Romania

Received: August 28, 2008 | Accepted: October 16, 2008

Introduction

The passage of wheels over agricultural soils, which is usually of short duration in the case of most vehicles, results in soil artificial compaction (Gill, 1968). The compaction phenomenon of agricultural soil can be defined as an increase in its dry density and the closer packing of solid particles or reduction in porosity (McKyes, 1985), which can result from natural causes, including rainfall impact, soaking and internal water tension (Gill, 1968; Arvidsson, 1997).

The most important factors that have a significant influence in the process of artificial compaction of agricultural soil are: the type of the soil, moisture content of the soil, intensity of external load, area of the contact surface between the soil and the tyre or track, shape of the contact surface, and the number of passes (Biriş, 2003).

Because the agricultural soil is not an homogeneous, isotropic, and ideal elastic material, the mathematical modelling of stress propagation phenomenon is very difficult. Many mathematical models of stress propagation in the soil under different traction devices are based on the Boussinesq equations, which describe the stress distribution under a load point (Figure 1) acting on a homogeneous, isotropic, semi-infinite, and ideal elastic medium (Hammel, 1994). Frohlich developed equations to account for stress concentration around the application point of a concentrated load for the problem of the half-space medium subjected to a vertical load (Kolen, 1983).

Many models of dynamic soil behaviour are using elastic properties of soil, and when the soil is represented by a linearly elastic, homogenous, isotropic, weightless material, the elastic properties required to fully account for the behaviour of the material are: Young's modulus (*E*), shear modulus (*G*), and Poisson's ratio (υ).

The Finite Element Method (FEM) is proving to be very promising for modelling this propagation phenomenon. For agricultural soils, the relationships between stresses and strains are measured on soil samples in the laboratory or directly in the field. The stress-strain relationships are given by constitutive equations (Gee-Clough, 1994).

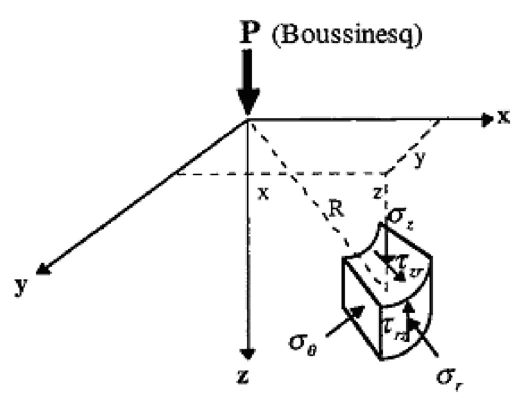

Figure 1. Stress state produced by a concentrated vertical load (Upadhyaya, 1997)

The main objective of this paper is to find and certify a mathematical model for prediction of the stress state in agricultural soil below tractors and machines tyres, using the most advanced mathematical tools, like Finite Element Method.

Material and methods

The Drucker-Prager plasticity model can be used to simulate the behaviour of agricultural soil. The yield criteria can be defined as:

$$F = 3 \cdot \alpha \cdot \sigma_m + \overline{\sigma} - k = 0 \tag{1}$$

where α and *k* are material constants which are assumed unchanged during the analysis, σ_m is the mean stress and $\overline{\sigma}$ is the effective stress, α and *k* are functions of two material parameters (Φ and *c*) obtained from the experiments, where Φ is the angle of internal friction and *c* is the material cohesion strength.

Using this material model, the following considerations should be noted: strains are assumed to be small; problems with large displacements can be handled providing that the small strains assumption is still valid; the use of NR (Newton-Raphson) iterative method is recommended; material parameters Φ and *c* must be bounded in the following ranges: 90≥ Φ ≥ 0 and c ≥ 0.

The required input parameters for the constitutive model of the agricultural soil of wet clay type are (Gee-Clough, 1994):

— Soil cohesion (*c*): 18.12 kPa
— Internal friction angle of soil (φ): 30
— Soil density (γ_w): 1270 kg/m^3
— Poisson's ratio (υ_s): 0.329
— Young's modulus (*E*): 3000 kPa

The stress levels under a point load as shown in Figure 1 are given in cylindrical coordinates as follows (Upadhyaya, 1997):

$$\sigma_z = \frac{3 \cdot P \cdot z^3}{2 \cdot \pi \cdot R^5} \tag{2}$$

$$\sigma_r = \frac{P \cdot z^3}{2 \cdot \pi} \cdot \left[\frac{3 \cdot z \cdot r^2}{R^5} - \frac{1 - 2 \cdot \upsilon}{R \cdot (R + z)} \right] \tag{3}$$

$$\sigma_\theta = \frac{P \cdot (1 - 2 \cdot \upsilon)}{2 \cdot \pi} \cdot \left[\frac{1}{R \cdot (R + z)} - \frac{z}{R^3} \right] \tag{4}$$

$$\tau_z = \frac{3 \cdot P \cdot r \cdot z^2}{2 \cdot \pi \cdot R^5} \tag{5}$$

where *P* –is the point load, υ -Poisson's ratio, $\sigma_{z,r,\theta}$ –normal stress components, and τ_{rz} –shear stress component.

Figure 2 shows the stress state in soil, of an infinitely cubic soil element, which can be written in a matrix, named the matrix of the stress tensors (Koolen, 1983). Stresses acting on a soil element can be described by mechanical invariants, which are independent of the choice of reference axes. The invariants yields are (Keller, 2004):

$$I_1 = \sigma_1 + \sigma_2 + \sigma_3 = \sigma_x + \sigma_y + \sigma_z \tag{6}$$

$$I_2 = \sigma_x\sigma_y + \sigma_x\sigma_z + \sigma_y\sigma_z - \tau_{xy}^2 - \tau_{xz}^2 - \tau_{yz}^2 = \\ = \sigma_1\sigma_2 + \sigma_1\sigma_3 + \sigma_2\sigma_3 \tag{7}$$

$$I_3 = \sigma_x\sigma_y\sigma_z + 2\tau_{xy}\,\tau_{xz}\,\tau_{yz} - \sigma_x\tau_{yz}^2 - \\ - \sigma_y\tau_{xz}^2 - \sigma_z\tau_{xy}^2 = \sigma_1\sigma_2\sigma_3 \tag{8}$$

It is useful to define the stress measures that are invariant. Such stress is the octahedral normal stress and the octahedral shear stress:

$$\sigma_{oct} = \frac{1}{3}(\sigma_1 + \sigma_2 + \sigma_3) = \frac{1}{3}I_1 \tag{9}$$

$$\tau_{oct} = \frac{1}{3}\sqrt{(\sigma_1-\sigma_2)^2 + (\sigma_2-\sigma_3)^2 + (\sigma_1-\sigma_3)^2} = \\ = \sqrt{\frac{2}{9}\cdot\left(I_1^2 - 3I_2\right)} \tag{10}$$

The critical state soil mechanics terminology uses the mean normal stress p and the deviator stress q. If $p=\sigma_{oct}$ (Eq. 9), q is given as (Keller, 2004):

$$q = \frac{1}{\sqrt{2}}\sqrt{(\sigma_1-\sigma_2)^2 + (\sigma_2-\sigma_3)^2 + (\sigma_1-\sigma_3)^2} = \\ = \sqrt{(I_1^2 - 3I_2)} \tag{11}$$

The incremental methods are used to deal with material and geometrically non-linear problems. The basis of the incremental procedure is the subdivision of the load into many small increments. Each increment is treated in a piecemeal linear behaviour with the stiffness matrix evaluated at the start of the increment. The tangent stiffness, E_t (Figure 3) for each element is calculated from the stress-strain curves according to the current stress level of that element. In a FEM calculation when the coordinates are continually updated the strain increment $d\in$ has the mean of a ratio between an incremental length and the current length.

The relationship between ε and $\in$ has the form (Gee-Clough, 1994):

$$\varepsilon = 1 - e^{-\in} \tag{12}$$

According to the relationship between ε and $\in$ the following revised stress-strain and tangent stiffness formulae were derived and used in the calculation (Gee-Clough, 1994):

$$\sigma_1 - \sigma_3 = \frac{1-e^{-\in_1}}{a + b\cdot(1-e^{-\in_1})} \tag{13}$$

$$E_t = \frac{1}{a}\cdot[1 - b\cdot(\sigma_1-\sigma_3)]\cdot[1-(b+a)\cdot(\sigma_1-\sigma_3)] \tag{14}$$

For saturated soil under an un-drained condition, the volume change is generally considered to be negligible. But for FEM calculation purposes, it is common to assume a constant Poisson's ratio slightly less than 0.5 (Gee-Clough, 1994). In terms of the concept of the incremental method, for a soil with nonlinear properties when increments are very small, Hooke's law in which the Young's modulus, E_t, and Poisson's ratio, υ_t, are variables (depending on current stress and strain values) is valid. On this basis, for a plane strain problem, a formula for the volume modulus, K_t, can be derived:

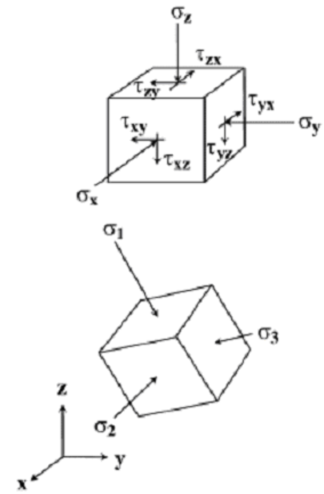

Figure 2.
Stress tensor components (Koolen, 1983)

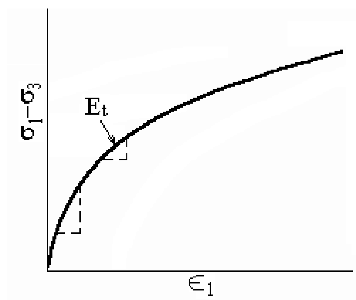

Figure 3.
Stress-strain curve for agricultural soil

$$K_t = \frac{d(\sigma_x+\sigma_y)}{d(\varepsilon_x+\varepsilon_y)} = \frac{E_t}{(1-\nu_t - 2\cdot\upsilon_t^2)} \tag{15}$$

where: ε_x, ε_y are strains in x and y directions; σ_x, σ_y are stresses in x and y directions.

If υ_t is constant, as E_t decreases (soil failure), K_t also decreases. This means that soil volume changes can be large. Assuming K_t is constant, and the initial values of E_t and υ_t are E_0 and υ_0, respectively, then the Poisson's ratio formula can be derived as in eq. (15) in which a maximum υ_t and a minimum E_t may be specified to avoid the calculation problem (Gee-Clough, 1994):

$$\upsilon_t = 0{,}25\cdot\left(\sqrt{9 - \frac{8\cdot E_t}{E_0}\cdot(1-\upsilon_0 - 2\cdot\upsilon_0^2)} - 1\right) \tag{16}$$

Figure 4 shows the theoretical shape of contact area between the soil and agricultural tyres. The pressure distribution along the width of tyre is described by a decay function (Keller, 2004):

$$p(y) = C \cdot \left[\frac{w(x)}{2} - y\right] \cdot e^{-\delta \cdot \left[\frac{w(x)}{2} - y\right]}; \; 0 \le y \le \frac{w(x)}{2} \quad (17)$$

and the pressure distribution in the driving direction is described by a power-law function:

$$p(x) = p_{x=0,y} \cdot \{1 - [\frac{x}{\frac{l(y)}{2}}]^{\alpha}\}; \; 0 \le x \le \frac{l(y)}{2} \quad (18)$$

where C, δ and α are parameters, $w(x)$ is the width of contact between the tyre and soil, $p_{x=0,y}$ is the pressure under the tyre centre and $l(y)$ is the length of contact between the tyre and soil.

Figure 5 shows the vertical load distribution in the contact area beneath agricultural tyres for three considerations: the real distribution with measured values (left), a model with uniform load distribution (centre), and a better model with irregular load distribution (right).

Equation (17) can describe different cases of pressure distribution, e.g. maximum pressure under the tyre centre or pressure under the tyre edge. The parameters C, δ and α are calculated from wheel load, tyre inflation pressure, recommended tyre inflation pressure at given wheel load, tyre width and overall diameter of the unloaded tyre. All these parameters are easy to measure or readily available from e.g. tyre catalogues.

Soil volume with the depth of 1 meter, the width of 3 meter and length of 4 meter (Figure 6) under the act of different tractors and harvester-threshers (Table 1) was considered. The structural nonlinear analysis was made on the ideal model, the soil being considered a homogeneous and isotropic material. The COSMOS/M 2.95 Programme was used for FEM modelling.

In order to check the model elaborated using FEM, laboratory tests were taken using a data acquisition system (Figure 7). The system was connected to Flexi Force Tekscan W-B201-L force sensors (Figure 8), vertically mounted in the soil, at 10 cm distance, in a metallic container with 1 x 1 x 1 m dimensions (Figure 9). The contact area shape of the wheels was reproduced and materialised using some metallic plates of 15 mm thickness. The load on the wheel in static state was applied using the Hidropuls equipment.

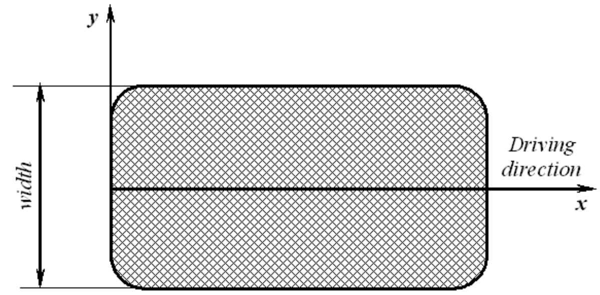

Figure 4. Shape of the contact surface between the soil and the tyre

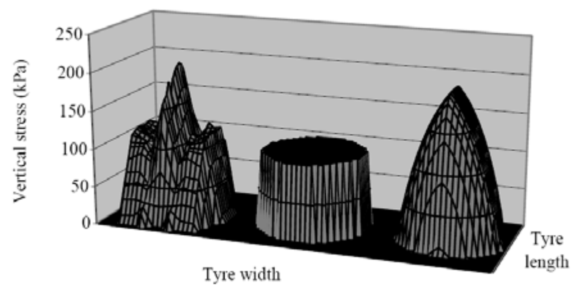

Figure 5. Distribution of the vertical load in the contact area (Keller, 2004)

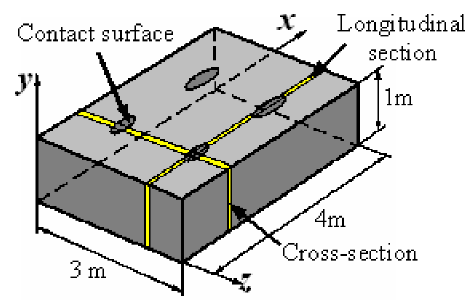

Figure 6. Analyzed soil volume

Table 1. The principal characteristics of the rolling devices used in modelling

Applicant	Soil interaction elements	Gauge [mm]	Mass (total/deck) [kg]		The active width for load, [mm]	Pressure on the soil, [kPa]
Romanian tractor U-445 (45 HP)	The front wheels	1500	1920	720	170	82.5
	The back wheels			1200	315	44.2
Romanian tractor U-650 (65 HP)	The front wheels	1600	3380	1170	180	110
	The back wheels			2210	367	57.3
Romanian Caterpillar SM-445 (45 HP)	Track	1300	2600		360	31
Harvester-thresher NH-TX66	The front wheels	2950	14000	11000	615	106.5
	The back wheels			3000	408	103.2
Romanian harvester-thresher Sema-140	The front wheels	2850	11033	9033	587	115
	The back wheels			2000	317.5	148.5

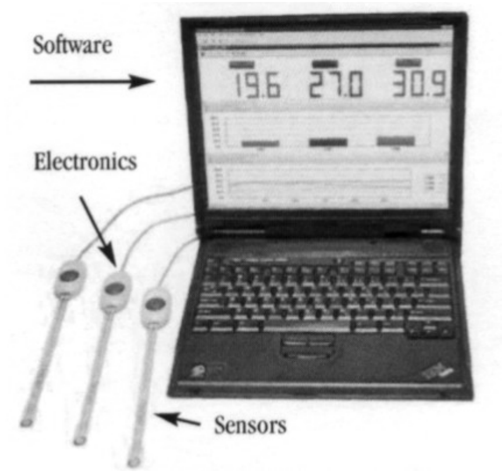

Figure 7. Data acquisition system

Figure 8. Flexi Force Tekscan W-B201-L force sensors

Figure 9. Metallic container

Results and discussion

Figures 10, 11, 12 and 13 show the results of FEM analysis in cross-section and in longitudinal section for two 45 HP tractors with tires and with caterpillar (U-445 and SM-445), respectively for two harvester-threshers (New Holland TX-66 and SEMA-140). These results are: the stresses distribution in soil and the graphical variation of stresses along the vertical-axial direction and along to the longitudinal direction.

In Figures 14 and 15 are comparatively presented the variation curves of the equivalent stresses with the points obtained by FEM calculus and by experimental tests for different depths along the tire's vertical axis in the case of the U-445 tractor.

Figure 16 shows the results of FEM analysis in cross-section for a "1/2 symmetrical model" which consists in equivalent stresses distribution in agricultural soil under the action of a uniform load in the case of back wheel of U-650 tractor.

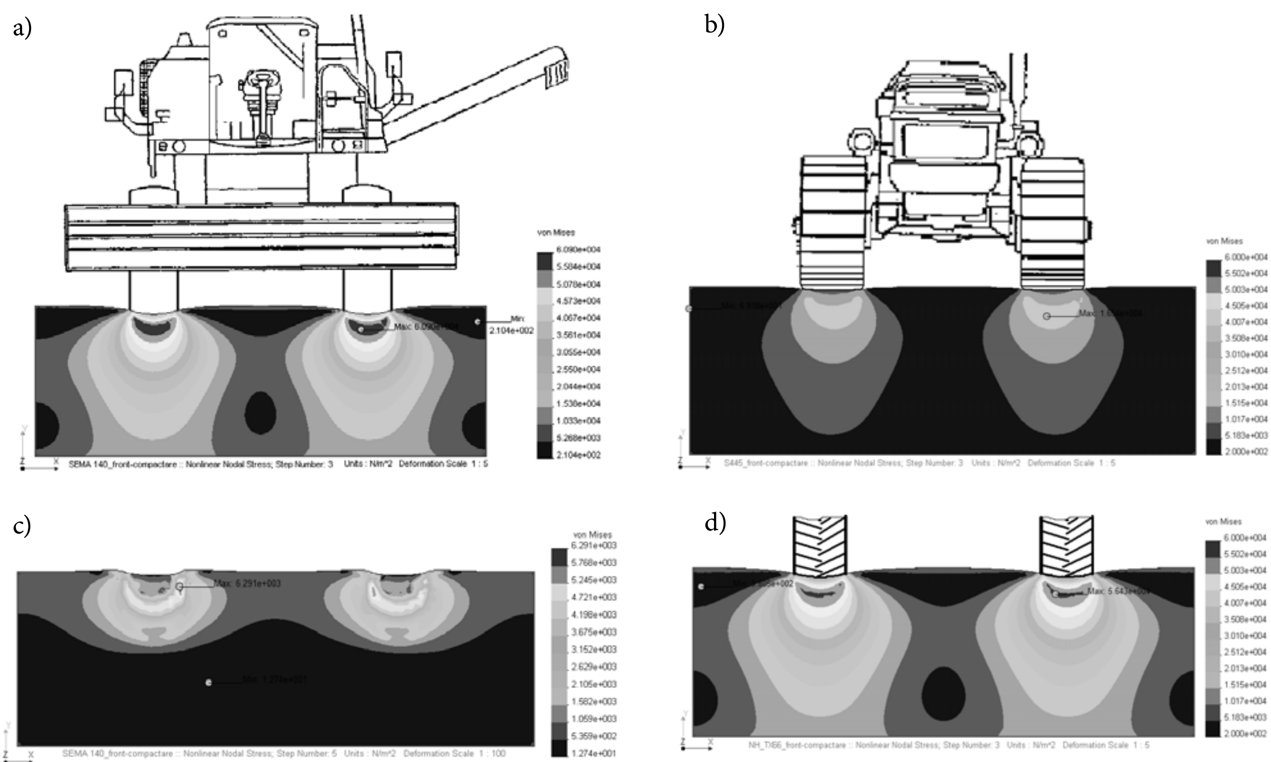

Figure 10. Stresses distribution in cross-section for: a) SEMA 140 harvester-thresher, b)SM-445 caterpillar tractor, c) SEMA 140 harvester-thresher after the first transit, d) New Holland TX-66 harvester-thresher (Units: Pa)

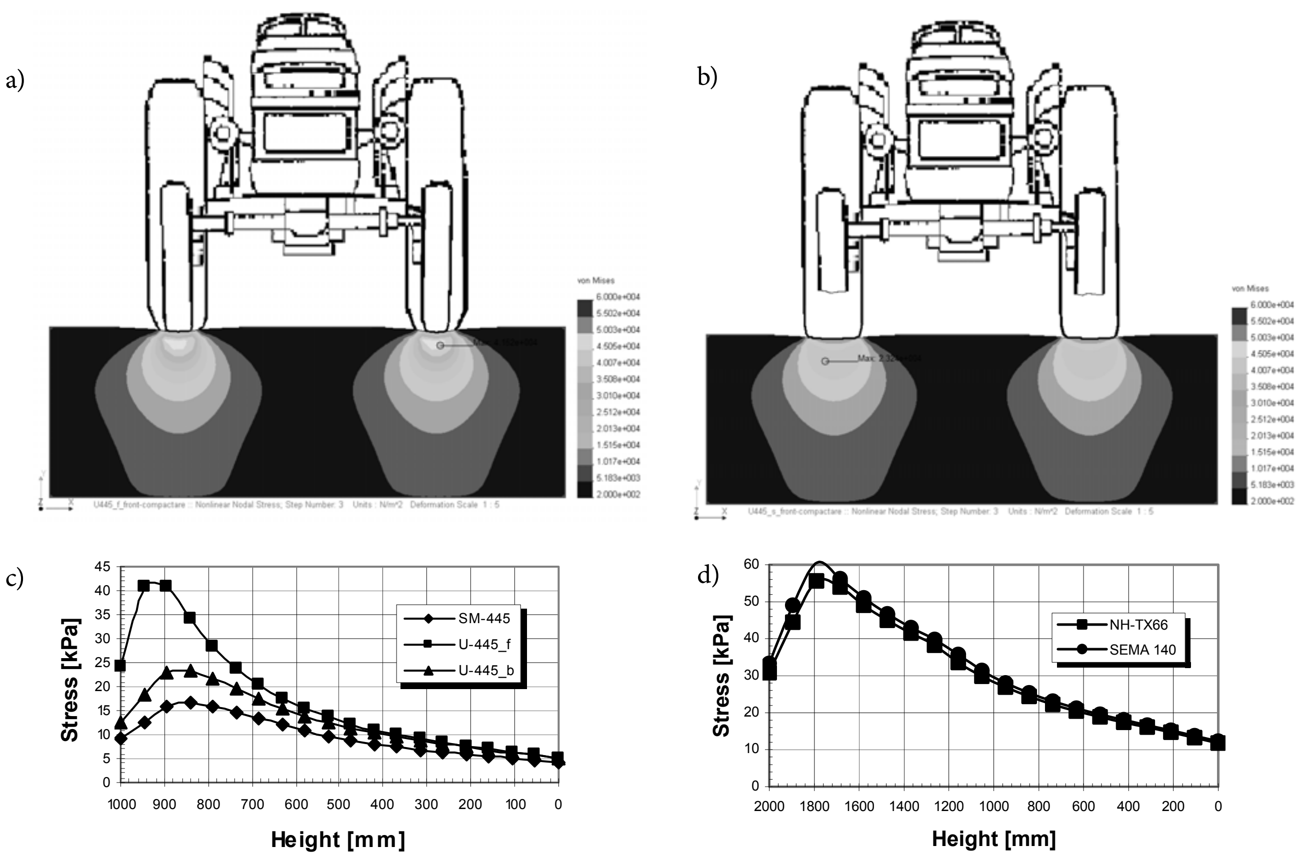

Figure 11. Stresses distribution in cross-section for: a) front wheels of U-445 tractor (U-445_f) (Units: Pa), b) back wheels of U-445 tractor (U-445_b) (Units: Pa), c-d) graphical distribution along the axial-vertical direction

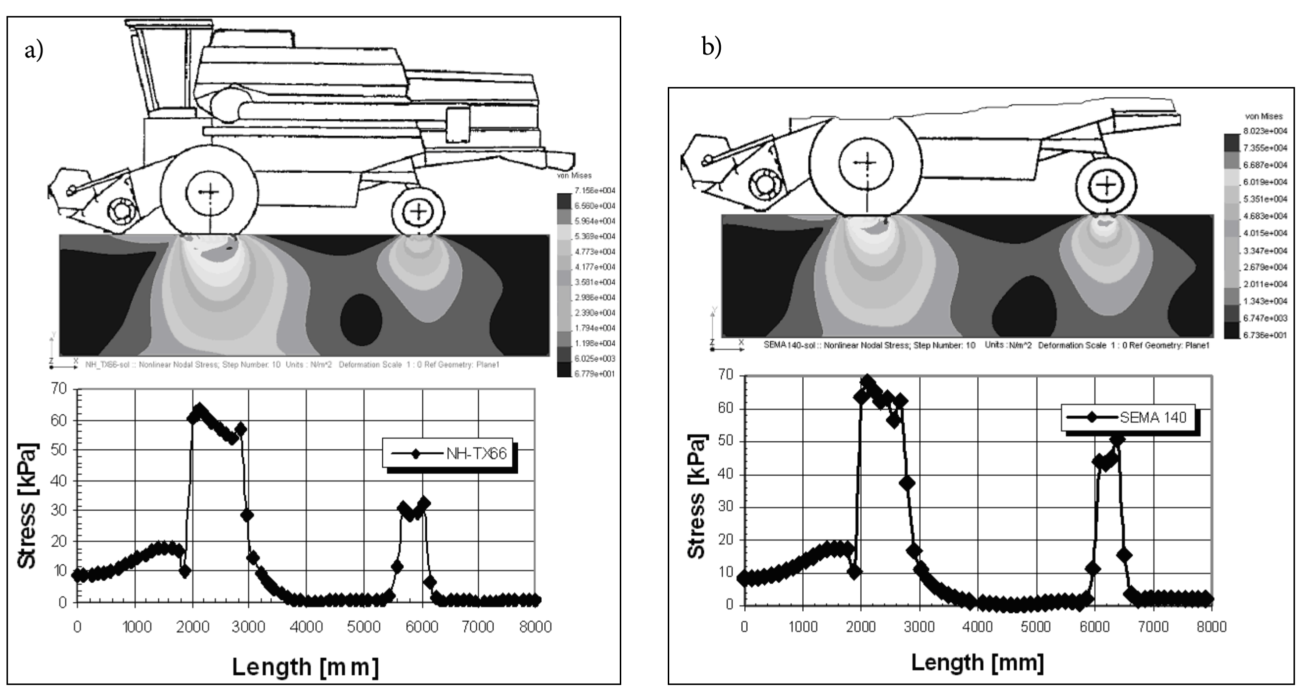

Figure 12. Stresses distribution and graphical variation along the longitudinal direction to the top layer of the soil in longitudinal section for: a) New Holland TX-66 harvester-thresher, b) SEMA 140 harvester-thresher

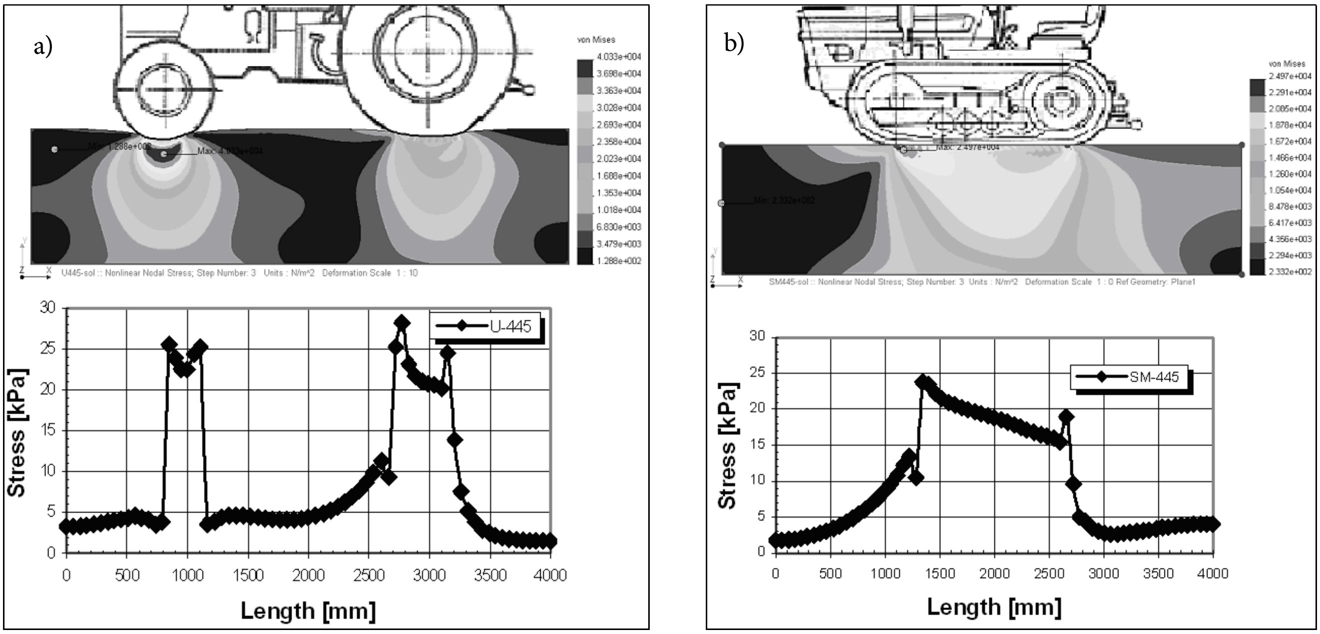

Figure 13. Stresses distribution and graphical variation along the longitudinal direction to the top layer of the soil in longitudinal section for: a) U-445 tractor, b) SM-445 caterpillar tractor

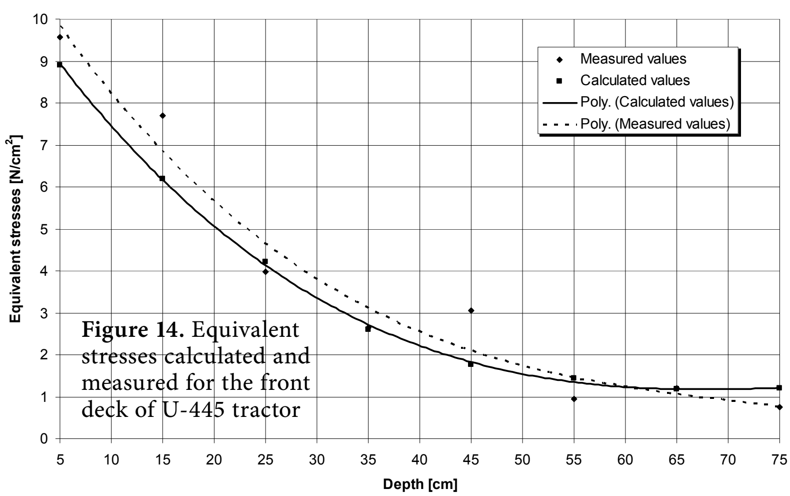

Figure 14. Equivalent stresses calculated and measured for the front deck of U-445 tractor

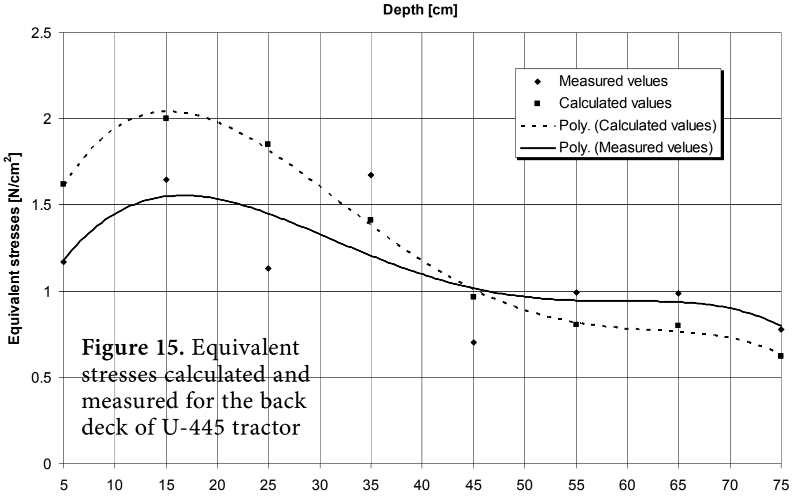

Figure 15. Equivalent stresses calculated and measured for the back deck of U-445 tractor

Figure 17 shows the distribution of equivalent stresses in agricultural soil in cross-section for the same "1/2 symmetrical model" under the action of an un-uniform load (Decay function) in the case of back wheel of U-650 tractor.

Figure 18 shows the graphical variation of equivalent stresses along the vertical-axial direction for the two cases of loading.

Conclusions

The Finite Element Method is in present the most advanced mathematical tool which can be used for the study of agricultural soil artificial compaction process. For mathematical modelling the soil is considered as a homogeneous and isotropic material, and the Drucker-Prager plasticity model can be used to simulate the behaviour of agricultural soil.

This study shows that, from these analysed tractors and harvester-threshers, the highest artificial compaction of soil was caused by the front wheels of SEMA-140 harvester-thresher (see Figure 11.d), when the equivalent maximum stress in soil is approx. 60 kPa, and in the case of the front wheels of NH TX-66 harvester-thresher, when the maximum equivalent stress is higher then 55 kPa. In these cases is recommended to extend the contact area between the wheel and the soil.

In the case of the front wheels of U-445 tractor (see figure 11.c), the equivalent maximum stress in soil is approximately 42 kPa. We can see that the equivalent maximum stress in soil in the case

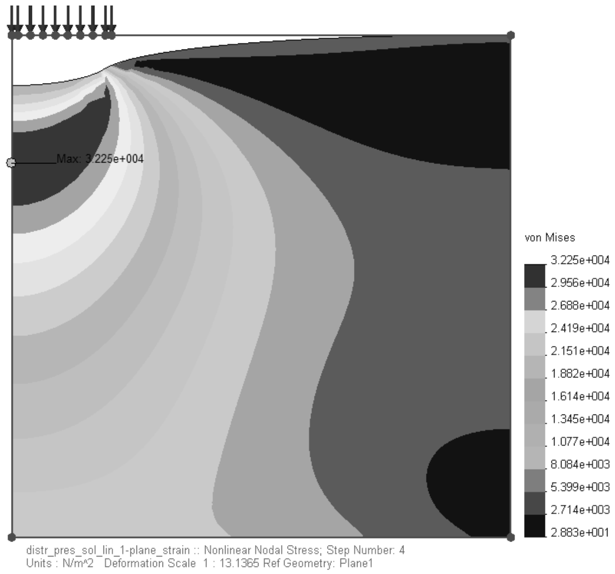

Figure 16. Distribution of equivalent stresses for uniform load in the case of back wheel of U-650 tractor (Units: Pa)

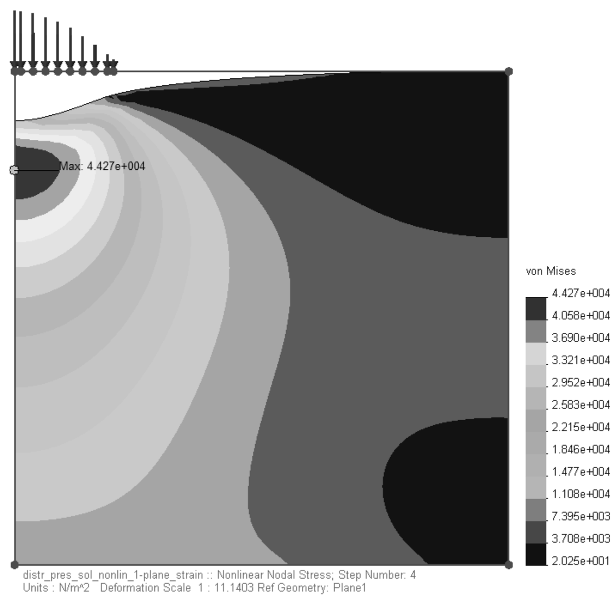

Figure 17. Distribution of equivalent stresses for un-linear load in the case of back wheel of U-650 tractor (Units: Pa)

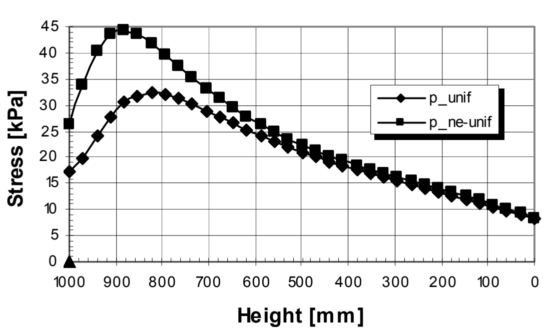

Figure 18. Graphical variation of stresses along the vertical-axial direction (p_unif: uniform load; p_ne-unif: un-linear load)

of analyzed caterpillar tractor (SM-445) is less than 20 kPa (Figure 11.c). This study represents a supplementary argument for using the caterpillar for the reduction of artificial soil compaction. The present researches are directed to using the rubber caterpillar, and also to using the reduce-pressure tyres with largest contact area with the soil.

We can see from the Figures 16, 17, and 18, that the distribution of equivalent stresses in soil volume is strongly influenced by the loading distribution in the contact area.

As we can see in Figure 14 and 15, between the calculated and measured results is a difference of 8 % for the front wheel and 12 % for the back wheel of U-650 tractor. There is a true development possibility of the pseudo-analytical procedures for the modelling of the stress propagation in agricultural soil, based on the work of Boussinesq, Fröhlich and Söhne, using the numerical calculus procedures, respectively the Finite Element Method.

References

Arvidsson J., (1997). Soil compaction in agriculture – from soil stress to plant stress, Doctoral Thesis, Agraria 41, Swedish University of Agricultural Sciences, Uppsala, Sweden.

Bailey A.C., Johnson C.E., Schafer R.L., (1986). A model for agricultural soil compaction, Journal of Agricultural Engineering Research, 33, 257-262.

Bakker D.M., Harris H.D., Wong, K.Y., (1995). Measurement of stress path under agricultural vehicles and their interpretation in critical state space, Journal of Agricultural Engineering, 61, 247-260.

Baumgartl T., Köck B., (2004). Modelling volume change and mechanical properties with hydraulic models, Soil Science Society of America Journal, 68, 57-65.

Biriş S.Şt., Prunău M., Vlăduţ V., Bungescu S.T., (2003). Study of agricultural soil artificial compaction using the finite element method, Scientific Bulletin of the „Politehnica" University of Timişoara, Transactions on Mechanics, Tomul 48(62), Fascicola 2, pp. 41-50.

Biriş S.Şt., Maican E., Bayer M., Vlăduţ V., Bungescu S., Prunău M., (2007). Advanced modelling of stress distribution in agricultural soil under different traction devices, Proceeding of the International Conference „Research people and actual task on multidisciplinary sciences", Bulgaria, Lozenec, 6-8 june, pp. 188-192.

Biriş S.Şt., Maican E., Faur N., Vlăduţ V., Bungescu S., (2007). FEM model for estimate of agricultural soil compaction risk, Proceeding of the 5th International Scientific and Practical Conference, Russia, Saint-Petersburg-Pavlovsk, 15-16 may, pp. 257-264.

Biriş S.Şt., Maican E., Faur N., Vlăduţ V., Bungescu S., (2007). FEM model for appreciation of soil compaction under the action of tractors and agricultural machines, Proceeding of the 35th International Symposium „Actual Tasks on Agricultural Engineering", Croatia, Opatija, 19-23 february, pp. 271-279.

Boussinesq J., (1885). Application des Potentiels à l'étude de l'équilibre et du Mouvement des Solides Élastiques, Gauthier-Villars, Paris, 30 pp.

Britto A.M., Gunn M.J., (1987). Critical State Soil Mechanics via Finite Elements, Ellis Horwood, Chichester, 488 pp.

Gee-Clough D., Wang J., Kanok-Nukulchai W., (1994). Deformation and Failure in Wet Clay Soil: Part 3, Finite Element Analysis of Cutting of Wet Clay by Tines, J. of Agric. Engng. Res. 58, pp. 121-131.

Gill W.R., Vandenberg G.E., (1968). Soil dynamics in tillage and traction, U.S.A. Department of Agriculture, Handbook 316, USA, Washington D.C.

Hammel K., (1994). Soil stress distribution under lugged tires, Soil and Tillage Research 32, pp. 163-181.

Horn R., Domzal H., Slowinska-Jurkiewicz A., Van Ouwerkerk C., (1995). Soil compaction process and their effects on the structure of arable soils and the environment, Soil and Tillage Research, 35, 23-36.

Keller T., (2004). Soil compaction and soil tillage - studies in agricultural soil mechanics, Doctoral Thesis. Agraria 489, Swedish University of Agricultural Sciences, Uppsala, Sweden.

Koolen A.J., Kuipers H., (1983). Agricultural soil mechanics, Advanced Series in Agricultural Sciences, Vol. 13. Springer, Heidelberg, 241 pp.

McKyes E., (1985). Soil cutting and tillage, Elsevier, Amsterdam-Oxford-New York-Tokyo.

O'Sullivan M.F., Henshall J.K., Dickson J.W., (1999). A simplified method for estimating soil compaction, Soil and Tillage Research, 49, 325-335.

Trautner A., (2003). On Soil Behaviour During Field Traffic, Doctoral Thesis, Agraria 372, Swedish University of Agricultural Sciences, Uppsala, Sweden.

Upadhyaya S.K., Rosa U.A., (1997). Prediction of traction and soil compaction, Proceeding of 3rd International Conference on Soil Dynamics. Tiberias, Israel, pp. 19-58.

Van den Akker J.J.H., (2004). SOCOMO: a soil compaction model to calculate soil stresses and the subsoil carrying capacity, Soil and Tillage Research 79, pp. 113-127.

Way T.R., Bailey A.C., Raper R.L., Burt E.C., (1995). Tire lug height effect on soil stresses and bulk density, Transactions of the American Society of Agricultural Engineers, 38, 669-674.

*** COSMOS/M – Finite Element System, User Guide, 1995.

acs74_04